From the design of bottom landfill liner systems to the impact assessment of contaminants on underlying aquifers

FROM THE DESIGN OF BOTTOM LANDFILL LINER SYSTEMS TO THE IMPACT ASSESSMENT OF CONTAMINANTS ON UNDERLYING AQUIFERS

by

Nicolò Guarena[1], Andrea Dominijanni[2] and Mario Manassero[3*]

[1] PhD Student, Department of Structural, Geotechnical and Building Engineering, Politecnico di Torino, Corso Duca degli Abruzzi 24, 10129 Torino (Italy); ORCID: 0000-0001-5576-2078; E-mail: nicolo.guarena@polito.it

[2] Associate Professor, Department of Structural, Geotechnical and Building Engineering, Politecnico di Torino, Corso Duca degli Abruzzi 24, 10129 Torino (Italy); ORCID: 0000-0002-0254-6002; E-mail: andrea.dominijanni@polito.it

[3] Full Professor, Department of Structural, Geotechnical and Building Engineering, Politecnico di Torino, Corso Duca degli Abruzzi 24, 10129 Torino (Italy); ORCID: 0000-0001-7621-5022; E-mail: mario.manassero@polito.it

[*] Corresponding Author

FROM THE DESIGN OF BOTTOM LANDFILL LINER SYSTEMS TO THE IMPACT ASSESSMENT OF CONTAMINANTS ON UNDERLYING AQUIFERS

ABSTRACT: The most recent advancements of the research activity that has been carried out at the Polytechnic University of Turin since the 90's are presented, with a focus on the design approaches which can be adopted for the optimisation of the engineered clay barriers that are used as a part of the composite liners of solid waste landfills. A particular attention is devoted to the characterisation of the geosynthetic clay liners (GCLs) in terms of their microstructural features and semipermeable properties, which affect both the liquid and contaminant transport and the swelling-shrinking behaviour upon a variation in the chemical and mechanical boundary conditions. In the first part of the paper, novel analytical solutions are derived in order to account for the influence of the chemico-osmotic counter-flow on the leakage rate through a lining system that consists of a geomembrane (GM) overlying a GCL, as well as for the effect of a variation in the GCL swelling pressure on the hydraulic transmissivity of the GM-GCL interface. In the second part of the paper, a steady-state analysis approach is proposed with the aim to include all the aforementioned phenomena in the assessment of the impact of contaminant migration through the landfill bottom liners on the groundwater quality, taking into account the presence of a natural attenuation layer (AL) between the GCL and the underlying aquifer.

Key Words: bentonite fabric, chemico-osmosis, geomembrane, geosynthetic clay liner, interface transmissivity, swelling pressure.

INTRODUCTION

The performance-based design of landfill lining systems requires the impact of contaminant migration from the waste on groundwater quality to be assessed. The effectiveness of lining systems is indeed demonstrated through the verification that the risk for human health and the environment due to the contaminant migration is limited to an acceptable level. This risk is quantified through the calculation of the contaminant concentration in the aquifer beneath the landfill, which is expected to remain less than some prescribed level at a compliance point, which is often a monitoring well located down-gradient from the landfill [8].

In order to conduct an analysis of the contaminant transport through the lining system of a landfill, the vertical mass flux of the contaminant must be determined taking into account the properties of all the layers interposed between the waste and the aquifer, including not only the engineered barriers, but also the natural foundation or attenuation layer (AL). As the regulations in force in most of the countries prescribe the use of a composite liner that consists of a geomembrane (GM) overlying a mineral liner, the advective component of the contaminant mass flux is controlled by the leakage rate through the holes that are created during the installation of the geomembrane, and during any subsequent construction activities, such as the placement of materials on top of the geomembrane. With regard to this matter, it is not possible not to mention the fundamental contribution given by J.P. Giroud to the understanding of the leakage mechanisms that govern the water migration through composite liners, as well as the development of a rational approach for the calculation of the leakage rate [16-20, 42].

This study is focused on the use of the geosynthetic clay liners (GCLs) in place of the compacted clay liners (CCLs) as the mineral components of the composite liners. GCLs consist of a thin layer of bentonite (5-10 mm thick) sandwiched between two geotextiles. The term “bentonite” is commonly used to indicate a clay soil with a high content (e.g. > 60%) of montmorillonite, a mineral of the smectite group that is constituted by thin lamellae characterised by a high specific

surface (defined as the surface per unit weight) and a permanent negative electric charge. The montmorillonite lamellae may aggregate in packets (also called tactoids), within which several clay platelets are in parallel array. As a result, the degree of aggregation in the bentonite micro-fabric may be quantified through the average number of lamellae per tactoid, $N_{l,AV}$, which can vary from 1 for a perfectly dispersed structure to values as high as 70-90 for highly aggregated structures [9].

As a consequence of the very high values of the specific surface which can be found in an ideal fully dispersed bentonite ($\simeq$ 780 m^2/g), the surface forces of electric nature are dominant over the mass forces (e.g. gravity) in these materials. The transport properties and the mechanical behaviour are therefore controlled by the electric interactions that occur at the micro-scale between the ions that are contained in the pore water and the clay particles. As a result of these interactions, bentonites may behave as semipermeable membranes, which are able to generate a water flux in response to a gradient in the chemical composition of the pore solution (chemico-osmosis). Moreover, bentonites may swell or shrink in response to changes in the chemical composition of the pore solution, as they are characterized by a macroscopic swelling pressure that is basically controlled by the solid skeleton fixed charge concentration of the clay particles [5, 26].

A theoretical approach for modelling the transport processes and the mechanical response of bentonites can be derived by upscaling the equations that govern the electric potential distribution, the water flow and the ion transport at the microscale. In such a theoretical approach the electric phenomena at the microscale are taken into account via a single parameter, $\overline{c}'_{sk,0}$, that represents the concentration of the solid skeleton electric charge [6, 7]. When this parameter is null, Terzaghi's equation for effective stress is recovered, as well as the standard advection-diffusion theory for solute transport; in all the other cases, the effective stress equation is modified to include the contribution of the swelling pressure, and the osmotic phenomena that characterize the behaviour of semipermeable membranes are incorporated in the water and solute flux equations [10]. $\overline{c}'_{sk,0}$ may be determined by fitting the experimental values of macroscopic parameters, such as the reflection

coefficient or the swell coefficient, which can be measured for different values of the salt concentration in the pore water or the bentonite void ratio [10, 12, 13, 31].

The changes in the solid skeleton electric charge, as well as in the hydraulic conductivity and the soil compressibility, which take place in response to the modifications of the bentonite fabric that are induced by large variations in the salt concentration of pore water or in the bentonite void ratio, are modelled through a Fabric Boundary Surface (FBS), whereby a fabric variable, such as $N_{l,AV}$, is related to the salt concentration, c_s, and the bentonite void ratio, e [11, 24, 28, 29]. The shape of the FBS is obtained by fitting the experimental data that are obtained through direct methods (e.g. transmission electron microscopy, X-ray diffraction analysis and nuclear magnetic resonance) or indirect methods (e.g. hydraulic conductivity test) for a specific bentonite [24].

As a result, starting from a limited number of laboratory tests, the mechanical behaviour and the transport properties of a bentonite under different conditions in terms of exposure to contaminants and applied external loads, is predicted through a theoretical model. From a practical standpoint this allows the barrier performances of GCLs to be simulated in a reliable way, taking into account the coupled hydro-chemo-mechanical behaviour of the bentonite.

In this study, an analytical solution for the calculation of the leakage rate through a composite liner that consists of a geomembrane overlying a geosynthetic clay liner is presented for the case of a hole that is located in correspondence of a wrinkle of the geomembrane. The solution contemplates the influence of the bentonite swelling on the determination of the hydraulic transmissivity at the interface between the geomembrane and the underlying geosynthetic clay liner, and the chemico-osmotic component of the water flow that is generated by the gradient in the solute concentration.

This solution is used to evaluate the vertical mass flux of the contaminant that is released in an aquifer beneath the landfill. The contaminant mass balance within the aquifer is used to calculate

97 the distribution of the contaminant concentration along the direction of the main component of
98 groundwater flux. The risk for human health and the environment may then be determined based on
99 the estimated value of the contaminant concentration [8].

100

101 **LEAKAGE RATE THROUGH GEOMEMBRANES OVERLYING GEOSYNTHETIC**
102 **CLAY LINERS**

103 The containment performance of composite liners that include a geomembrane over a low-
104 permeability mineral layer is highly affected by the areal density of wrinkles in the geomembrane,
105 whose formation is mostly controlled, during the liner construction, by the thermal expansion of the
106 geomembrane upon heating by solar radiation, as well as by its placement and protection
107 procedures. Apart from the case of volatile organic compounds, which are able to readily pass
108 through intact polymer-based barriers via molecular diffusion [39], the vast majority of inorganic
109 pollutants have been observed to migrate through the holes of geomembranes, and preferentially
110 through holes that are located in correspondence of wrinkles rather than holes that occur in flat
111 areas, as the transmissivity of the gap beneath the wrinkle is generally much higher that the
112 transmissivity of the zone between the geomembrane and the underlying mineral layer [35, 36].

113 Among the different approaches that have been proposed with the aim to evaluate the rate of
114 leachate flow through a defect in a geomembrane overlying a mineral layer [15, 20, 42], the general
115 framework studied by Rowe [35] and Touze-Foltz et al. [43] for a circular hole in a flat
116 geomembrane and for a damaged wrinkle is here adopted in order to extend the existing analytical
117 solutions to the case of clay layers with a high content of smectite minerals, such as the
118 geosynthetic clay liners, which are able to exhibit semipermeable membrane behaviour when
119 permeated with diluted solutions. Such an extension is carried out only for the case of a damaged
120 wrinkle (i.e. the “two-dimensional case”), as it is the one of greatest concern with respect to the

problem of estimating the rate of contaminant transport through the bottom liners of waste disposal facilities.

Effect of the chemico-osmosis on the liquid flow through GM-GCL interfaces

The idealised scenario considered hereafter is depicted in Figure 1. The liquid that has infiltrated through the geomembrane hole is assumed to spread horizontally and perpendicularly to the longitudinal axis of the wrinkle within the GM-GCL interface, which is hypothesised to be characterised by a uniform hydraulic transmissivity, θ, up to a distance that is referred to as the half width of the wetted area, ξ_w. Finally, the liquid migrates vertically through the mineral layer.

Under fully saturated conditions and assuming that the length of the damaged wrinkle, L_w, is much larger than its half width, b_w, the boundary effects at the ends of the wrinkle can be neglected and the horizontal liquid flow rate in the transmissive zone, Q_ξ, is given by:

$$Q_\xi = -L_w \theta \frac{\mathrm{d}h}{\mathrm{d}\xi} \tag{1}$$

where h is the pressure head in the GM-GCL interface.

On the basis of the theoretical model developed by Dominijanni and Manassero [7], the vertical liquid flow rate, Q_s, which infiltrates into the strip of the geosynthetic clay liner between the coordinates ξ and $\xi + \mathrm{d}\xi$ can be regarded as the superposition of a Darcian component, which is driven by the gradient in hydraulic head, and a chemico-osmotic component, which is driven by the gradient in concentration of the inorganic contaminant across the semipermeable clay layer:

$$\mathrm{d}Q_s = k_g \frac{H_g + h - h_b}{H_g} L_w \mathrm{d}\xi - 2RT \frac{k_g}{\gamma_w} \omega_g \frac{c_p - c_b}{H_g} L_w \mathrm{d}\xi \tag{2}$$

where k_g is the hydraulic conductivity of the geosynthetic clay liner, H_g is the thickness of the geosynthetic clay liner, h_b is the pressure head at the bottom of the geosynthetic clay liner, R is the

universal gas constant (8.314 $J \cdot mol^{-1} \cdot K^{-1}$), T is the absolute temperature, γ_w is the water unit weight (γ_w = 9.81 kN/m^3), ω_g is the reflection coefficient or chemico-osmotic efficiency coefficient, c_p is the contaminant concentration in the leachate collection and removal system and c_b is the contaminant concentration at the bottom of the geosynthetic clay liner.

The reflection coefficient quantifies the ability of the geosynthetic clay liner to act as a selectively permeable membrane, and usually varies from zero for non-semipermeable porous media to unity for "ideal" semipermeable porous media, whose conductive pores cannot be accessed by the negatively charged ion species (i.e. the anions that result from the dissociation of the contaminant in solution). When the contaminant of interest consists of a 1:1 electrolyte, a closed-form expression of the reflection coefficient can be provided [12]:

$$\omega_g = 1 + \frac{\vec{c}'_{sk,0}}{2e\left(c_p - c_b\right)}\left[Z_2 - Z_1 - (2t_1 - 1)\ln\left(\frac{Z_2 + 2t_1 - 1}{Z_1 + 2t_1 - 1}\right)\right] \tag{3}$$

where $\vec{c}'_{sk,0}$ is the solid charge coefficient, e is the void ratio of the bentonite component of the geosynthetic clay liner and the dimensionless parameters Z_1, Z_2 and t_1 are given by:

$$Z_1 = \sqrt{1 + \left(\frac{2c_p e}{\vec{c}'_{sk,0}}\right)^2} \tag{4}$$

$$Z_2 = \sqrt{1 + \left(\frac{2c_b e}{\vec{c}'_{sk,0}}\right)^2} \tag{5}$$

$$t_1 = \frac{D_{1,0}}{D_{1,0} + D_{2,0}} \tag{6}$$

being $D_{1,0}$ and $D_{2,0}$ the free-solution or aqueous-phase diffusion coefficients of the cation and the anion, respectively.

160 The following equation correlates the solid charge coefficient with the bentonite cation
161 exchange capacity, CEC, which should be measured by means of experimental procedures that
162 allow a complete dispersion of the bentonite unit layers, or montmorillonite lamellae, to be achieved
163 [13]:

164 $$\overline{c}'_{sk,0} = \frac{1 - f_{Stern}}{N_{l,AV}} \cdot \mathrm{CEC} \cdot \rho_{sk} \cdot \frac{e}{e_m} \tag{7}$$

165 where f_{Stern} is the fraction of the adsorbed cations that are immobilised in the so-called Stern layer
166 ($f_{Stern} \simeq 0.85$), as opposed to the adsorbed cations that are delocalised in the diffuse-ion swarm
167 surrounding the bentonite particle or tactoid [40], ρ_{sk} is the solid-phase density ($\rho_{sk} \simeq 2.65$ kg/dm^3),
168 $N_{l,AV}$ is the average number of montmorillonite lamellae that form the tactoid and e_m is the micro-
169 void ratio which, according to a simplified dual-porosity scheme of the bentonite fabric wherein the
170 tactoid consists of a parallel stacking of montmorillonite lamellae [32, 41], represents the portion of
171 the void ratio comprising the inter-tactoid conductive pores [24]:

172 $$e_m = e - b_n \rho_{sk} \mathrm{CEC} \frac{F}{\sigma} \left(\frac{N_l - 1 + d_d}{N_l} \right) \tag{8}$$

173 being b_n the average half distance between the montmorillonite lamellae in the tactoid ($b_n \simeq 0.45$
174 nm), d_d the ratio of the Stern layer thickness to the half inter-lamellar distance ($d_d \simeq 4$), F the
175 Faraday constant (F = 96487 C/mol) and σ the surface density of the solid skeleton electric charge
176 (σ = 0.114 C/m^2).

177 The pressure head profile in the GM-GCL interface can be determined by accounting for the
178 following mass conservation equation:

179 $$\mathrm{d}Q_s + \frac{\mathrm{d}Q_\xi}{\mathrm{d}\xi} \mathrm{d}\xi = 0 \tag{9}$$

Substitution of Equations 1 and 2 into Equation 9 leads to a second order linear non-homogeneous differential equation with constant coefficients, which can be solved in conjunction with the following boundary conditions [43]:

$$\begin{cases} h\left(\xi = b_w\right) = h_p \\ h\left(\xi = \xi_w\right) = 0 \\ \dfrac{\mathrm{d}h}{\mathrm{d}\xi}\left(\xi = \xi_w\right) = 0 \end{cases} \tag{10}$$

The pressure head profile in the GM-GCL interface, the half width of the wetted area and the vertical liquid flow rate infiltrating into the composite liner for a single damaged wrinkle are then given by:

$$h = 2G\sinh^2\left[\alpha\left(\frac{\xi_w - \xi}{2}\right)\right] \tag{11}$$

$$\xi_w = b_w + \frac{1}{\alpha}\cosh^{-1}\left(1 + \frac{h_p}{G}\right) \tag{12}$$

$$Q_s = 2\frac{k_g}{H_g}L_w\int_0^{\xi_w}\left(h+G\right)\mathrm{d}\xi = 2\frac{k_g}{H_g}L_w b_w G\left\{1 + \frac{h_p}{G} + \frac{1}{b_w\alpha}\sinh\left[\alpha\left(\xi_w - b_w\right)\right]\right\} \tag{13}$$

where the parameters G and α are expressed as follows:

$$G = H_g - h_b - h_\pi \tag{14}$$

$$\alpha = \sqrt{\frac{k_g}{H_g\theta}} \tag{15}$$

193 The term h_π in Equation 14 is referred to as the osmotic head and depends on the
194 semipermeable properties of the geosynthetic clay liner, as well as on the difference in contaminant
195 concentration between the GCL boundaries:

196 $$h_\pi = 2RT\frac{\omega_g}{\gamma_w}\left(c_p - c_b\right) \tag{16}$$

197 The derived analytical expressions for h, ξ_w and Q_s are valid if $G > 0$ (i.e. $h_\pi < H_g - h_b$); at the
198 limit $G \rightarrow 0^+$, the half width of the wetted area tends to infinity. As the thickness of geosynthetic
199 clay liners can be assumed, as a first approximation, equal to 0.01 m and the osmotic head can
200 easily reach values of the order of 0.1 m, the proposed theoretical model results to be of practical
201 utility for the design of composite liners when the pressure head at the bottom of the geosynthetic
202 clay liner assumes negative values (i.e. $h_b < 0$), that is, when a matric suction builds up without a
203 change in the saturation degree. Finally, it is stressed that the derived analytical solution is valid if
204 the spacing between two adjacent wrinkles in the geomembrane, l_w, is large enough to avoid any
205 mutual interaction, and therefore it should be verified that the condition $\xi_w < 0.5\ l_w$ is satisfied.

206 As exemplified in Figures 2 and 3 for a set of representative values of the parameters b_w, h_p,
207 H_g and h_b [37], an increase in the osmotic head produces an increase in the half width of the wetted
208 area and a decrease in the liquid flow rate through a single damaged wrinkle, thus highlighting the
209 improvement in the containment performance of the composite liner due to the GCL membrane
210 behaviour. In addition to the advantages that arise from the chemico-osmotic counter-flow, also the
211 hydraulic transmissivity of the GM-GCL interface significantly influences the resulting leachate
212 flow rate through the composite liner [30, 35], as a variation in the θ parameter affects the value
213 that is assumed by the α parameter; the latter remark has therefore stimulated further investigation
214 on the relationship that exists between the bentonite osmotic properties and the GM-GCL interface
215 transmissivity.

Effect of the bentonite swelling behaviour on the GM-GCL interface transmissivity

Although a number of studies have focused on the experimental assessment of the GM-GCL interface transmissivity by addressing the issue of the influence that is exerted, for instance, by the vertical confining stress, the bentonite gradation (powdered and granular), the cover geotextile fabric (woven and non-woven), the hydraulic head and the GCL prehydration, few of them have investigated the effect that is related to the physico-chemical interactions which occur between the bentonite component of the geosynthetic clay liner and the permeating solution: such pore-scale interactions, which are responsible for the semipermeable membrane behaviour, also affect the mechanical behaviour of bentonites and, in particular, the swelling-shrinking response upon a variation in the chemical composition of the permeant [31]. As discussed by AbdelRazek and Rowe [1], exposure of the geosynthetic clay liner to solutions with high ionic strength can alter the swelling ability of the bentonite and, consequently, its ability to conform to the irregularities at the interface between the geomembrane and the GCL cover geotextile, with an increase in the hydraulic transmissivity compared to permeation with deionised water.

On the basis of the same modelling assumptions that were adopted by Dominijanni and Manassero [7] to simulate the coupled flows of solvent and solutes through electrically charged porous media, it is possible to provide a closed-form expression of the chemico-osmotic swelling pressure, u_{sw}, when the inorganic contaminant of interest consists of a 1:1 electrolyte [12]:

$$u_{sw} = 2RTc_{avg}\left[\sqrt{\left(\frac{\bar{c}'_{sk,0}}{2ec_{avg}}\right)^2 + 1} - 1\right] \tag{17}$$

where c_{avg} can be assumed equal to the arithmetic mean of the values of the contaminant concentration at the GCL boundaries:

$$c_{avg} = \frac{c_p + c_b}{2} \tag{18}$$

238 Mendes et al. [30] were the first to carry out laboratory tests aimed at investigating how the
239 GM-GCL interface transmissivity is affected by cation exchange phenomena, whereby sodium
240 cations which initially represent the dominant ion species in the exchange complex of the bentonite
241 are replaced by multivalent cations. Four different GCLs, which consisted of either sodium
242 bentonite or calcium bentonite, were tested and the obtained results, in terms of measured liquid
243 flow rate through the composite liner system, were interpreted by means of the analytical solution
244 proposed by Touze-Foltz et al. [43] for a circular hole in a flat geomembrane (i.e. the "axi-
245 symmetric case"). In spite of a variation in the GCL hydraulic conductivity up to three orders of
246 magnitude, the composition of the exchange complex of the bentonite was not observed to
247 significantly influence the GM-GCL interface transmissivity at steady-state conditions; however, it
248 is not possible to draw conclusions about the impact of the chemistry of the pore solution on the θ
249 parameter, as clean water was used as the permeant during the tests.

250 Rowe and Abdelatty [38] carried out a series of laboratory tests on a composite liner system
251 by circulating both reverse osmosis water and a 0.14 M NaCl solution, which resulted in an increase
252 in the GLC hydraulic conductivity by about an order of magnitude and in an almost unchanged
253 liquid flow rate. On the basis of a numerical interpretation of the aforementioned results, it was
254 concluded that the GM-GCL transmissivity had to experience a twofold decrease as a consequence
255 of the physico-chemical interactions between the geosynthetic clay liner and the salt solution.

256 Among the tests series that were performed by AbdelRazek and Rowe [1] with the aim to
257 investigate the effect of a number of variables on the GM-GCL interface transmissivity, two of
258 them focused on the measurement of the θ parameter upon permeation of a coated needle-punched
259 GCL, placed in contact with a smooth 1.5 mm-thick HDPE GM, by reverse osmosis water (I < 3.29
260 mM), a synthetic MSW landfill leachate (I = 159.5 mM) and a saline solution (I = 4400 mM), being
261 I the ionic strength of the permeant, under vertical confining stresses ranging between 10 and 150
262 kPa. All tests were carried out with an novel experimental apparatus, which forces the liquid to

spread horizontally at the GM-GCL interface rather than vertically through the GCL: as a difference from the aforementioned studies, the estimation of the θ parameter is the result of a direct measurement, and not of an interpretation that, necessarily, involves a number of modelling hypotheses. The reported trends in the steady-state values of the interface transmissivity versus the ionic strength of the permeant are consistent with the available experimental evidences on the osmotic swelling of clay soils [4, 12, 33], as permeation with both the synthetic leachate and the saline solution was detrimental with respect to the bentonite swelling potential and, consequently, to the GM-GCL interface transmissivity, which increased up to four orders of magnitude at the lowest confining stress compared to permeation with reverse osmosis water. Nevertheless, further analysis of these experimental results through Equation 17 is not possible, since AbdelRazek and Rowe [1] did not provide sufficient data concerning the tested GCL (e.g. the GCL hydraulic conductivity) for a direct or indirect evaluation of the fundamental fabric parameter (i.e. the average number of lamellae per tactoid, $N_{l,AV}$), which accounts for the arrangement of the bentonite unit layers at the microscale and influences the effective electric charge concentration of the solid phase [24].

AbdelRazek and Rowe [2] carried out additional tests series by means of the same testing apparatus described by AbdelRazek and Rowe [1], with the aim to investigate the effect determined by the permeation of an untreated and a polymer-enhanced GCL (without smooth and indented coating or lamination) with a saline solution on the GM-GCL interface transmissivity. With reference to the polymer-enhanced GCL that was tested in contact with a smooth 2 mm-thick LLDPE GM, two permeants were used, namely reverse osmosis water (I < 3.29 mM) and a saline solution with varying ionic strength (I = 440 - 2200 - 4400 mM), at two different confining stress levels (σ_v = 10 - 150 kPa). Upon termination of the interface transmissivity tests, the GCL hydraulic conductivity was measured in a flexible wall permeameter and a weak dependence of k_g on the brine concentration emerged from the tests results, which are listed in Table 1. Such results are here

interpreted through the modified Kozeny-Carman equation, which relates the GCL hydraulic conductivity to the average number of lamellae per tactoid [29]:

$$k_g = \frac{\tau_m}{3}\frac{\gamma_w}{\mu_e}\frac{e_m^3}{(1+e_m)}\left(\frac{\sigma}{F\rho_{sk}\mathrm{CEC}}\right)^2 N_{l,AV}^2 \tag{19}$$

where τ_m is the matrix tortuosity factor, which accounts for the tortuous nature of the actual flow paths within the bentonite pores ($\tau_m \simeq 0.2$), and μ_e is the electro-viscous coefficient that, as a first approximation, can be assumed equal to the viscous coefficient of water ($\mu_e \simeq 1$ mPa·s). The CEC of the tested GCL was measured to be 83 meq/100g.

The calculated values of the $N_{l,AV}$ parameter, which are listed in Table 1, allow the influence of the ionic strength of the permeant on the clay fabric to be appreciated, whose aggregation state did not significantly change from one to another test, thus demonstrating the effectiveness of the polymer enhancement in maintaining a dispersed microstructure of the bentonite. The calculated $N_{l,AV}$ values are also plotted in Figure 4 as a function of the micro-void ratio, together with the iso-concentration curves (i.e. curves of equal ionic strength of the permeant) of the Fabric Boundary Surface, as was calibrated by Manassero [24] on the basis of the results of the hydraulic conductivity tests performed by Petrov and Rowe [34] on an untreated needle-punched GCL (without polymer addition). The phenomenological equation of the Fabric Boundary Surface is given as follows:

$$N_{l,AV} = N_{l,AV0} + \frac{\alpha}{e_m}\left(\frac{c_{avg}}{c_0}+1\right) + \beta e_m\left[1-\exp\left(-\frac{c_{avg}}{c_0}\right)\right] \tag{20}$$

where c_0 is the reference concentration (c_0 = 1 M) and $N_{l,AV0}$ is the ideal average minimum number of lamellae per tactoid when c_{avg} = 0 and $e_m \rightarrow \infty$. The dimensionless coefficients α, β and $N_{l,AV0}$ have to be regarded as material-dependent parameters and, therefore, should be adjusted on a given set of data pertaining to a specific bentonite ($N_{l,AV0}$ = 1.56, α = 8.82 and β = 10.01 for the GCL

309 tested by Petrov and Rowe [34]). When the permeating solution consists of a mixture of ion species,
310 as in the case of the tests series carried out by AbdelRazek and Rowe [2], the average contaminant
311 concentration across the GCL (see Equation 18) can be set equal to the ionic strength.

312 Figure 4 draws attention to the different behaviours of the modified GCL tested by
313 AbdelRazek and Rowe [2] and the untreated GCL tested by Petrov and Rowe [34]. Indeed, whilst
314 the bentonite aggregation state does not appreciably change upon permeation with diluted solutions,
315 the difference in $N_{l,AV}$ between the two GCL types becomes more and more pronounced as the ionic
316 strength increases: such bentonite flocculation phenomena for the untreated GCL led to an increase
317 in the measured hydraulic conductivity up to three orders of magnitude moving from a 10 mM to a
318 2000 mM NaCl solution.

319 In order to investigate the influence of the bentonite osmotic swelling on the GM-GCL
320 interface transmissivity, a value of the swelling pressure has been calculated through Equation 17
321 for each measured steady-state value of θ (Table 2), adopting the arithmetic mean of the $N_{l,AV}$ values
322 listed in Table 1 (i.e. $N_{l,AV}$ = 7.21) and the ionic strength of the permeant in lieu of the 1:1
323 electrolyte concentration. The first of the previous assumptions is acceptable for the considered
324 GCL, as clay fabric modifications were substantially hindered by the polymer enhancement, with a
325 narrow range of variation in the $N_{l,AV}$ parameter ($N_{l,AV}$ = 2.64 - 12.46). As far as the second
326 assumption is concerned, it is noted that the osmotic swelling-shrinking behaviour of bentonites is
327 mostly controlled by the Debye length which, in turn, is inversely proportional to the square root of
328 the ionic strength of the permeant [22]: in the simplest case of a single 1:1 electrolyte, the ionic
329 strength equals the electrolyte concentration but, in the most general case, it allows the detrimental
330 effect of the presence of multivalent cations to be taken into account when calculating the chemico-
331 osmotic swelling pressure through Equation 17.

332 Consistently to the diffuse double layer theory, the swelling pressure is found to be relevant
333 only in case of permeation with reverse osmosis water, being almost completely annulled in case of

334 permeation with highly concentrated saline solutions. With respect to the latter case, as observed by
335 AbdelRazek and Rowe [2], there is no clear trend between the interface transmissivity and the
336 vertical confining stress, thus suggesting that the variability in GCL specimens and GM-GCL
337 contact conditions dominated the measured liquid flow and did not allow the influence of the stress
338 level to be appreciated. On the contrary, when the GCL is permeated by reverse osmosis water, the
339 increase in the swelling pressure resulting from a decrease in the bentonite void ratio, which in turn
340 is related to a change in the vertical confining stress, seems to correlate well with the reduction in
341 the interface transmissivity and, on the basis of such a remark, an attempt has been made in order to
342 define a first tentative empirically-based relationship between the GM-GCL interface transmissivity
343 and the bentonite swelling pressure for the composite liner system which was tested by AbdelRazek
344 and Rowe [2], as illustrated in Figure 5. In particular, the curve that interpolates the two available
345 experimental data measured with reverse osmosis water is given by:

346 $$\log_{10}\theta = -9.553 - 0.04121 \cdot u_{sw} \quad (21)$$

347 where θ and u_{sw} are expressed in m^2/s and kPa, respectively.

348 Further research is warranted in order to investigate the influence of a variation in the stress
349 level on the interface transmissivity, especially when the swelling pressure is annulled as a
350 consequence of permeation with highly concentrated solutions. Moreover, the derived empirical
351 equation should be considered valid only in case of monotonic loadings, for which a unique σ_v - e
352 relationship may exist, thus excluding any preconsolidation effect.

353

354 **IMPACT OF CONTAMINANT MIGRATION THROUGH LANDFILL BOTTOM LINERS**
355 **ON THE GROUNDWATER QUALITY**

356 The idealised scenario which is considered for the evaluation of the effectiveness of landfill
357 bottom liners in limiting the migration of inorganic contaminants from the waste fill is depicted in
358 Figure 6. It is assumed that the pollutant of interest, which consists of an electrolyte completely
359 dissolved in water, migrates vertically from the leachate collection and removal system towards the
360 underlying aquifer through the composite liner, which is constituted by a geomembrane (GM)
361 overlying a geosynthetic clay liner (GCL). A natural attenuation layer (AL), which is characterised
362 by a higher hydraulic conductivity than the engineered clay barrier, is interposed between the
363 aquifer and the composite liner: such a low-permeability foundation layer is meant to reduce the
364 concentration gradient along the contaminant migration path and, as a result, the rate of diffusive
365 transport from the waste fill [39]. When the pollutant reaches the aquifer, which is hypothesised to
366 be sufficiently thin in order to neglect the vertical distribution of the contaminant concentration in
367 the groundwater, advection becomes the main transport mechanism in the horizontal direction
368 compared to longitudinal hydrodynamic dispersion.

369 The analytical solution that is presented hereafter is developed under the assumptions of
370 steady-state conditions and constant source concentration in the waste leachate, as done for instance
371 by Guyonnet et al. [21] and Foose [14]. In particular, with respect to the already available steady-
372 state analysis approach proposed by Dominijanni and Manassero [8] to model the impact of
373 contaminant migration from the waste fill on the groundwater quality, this paper aims to extend
374 such an analysis tool in order to account for the bentonite semipermeable properties, which are
375 responsible for the improvement of the GCL containment performance as a result of three processes
376 that reduce the pollutant mass flux, namely hyperfiltration, chemico-osmotic counter-advection and
377 restricted diffusion [23].

378 First of all, under the hypothesis of thin aquifer (i.e. aquifer thickness, H_{aq}, of the order of few
379 meters), solving the balance equation for the volumetric liquid flux inside the aquifer yields the

following linear relationship between the horizontal groundwater flux, q_x, and the horizontal distance beneath the landfill in the direction of the groundwater flow, x [8]:

$$q_x = q_{x0} + \frac{q_c}{H_{aq}} x \tag{22}$$

where q_{x0} is the groundwater flux just upstream from the landfill and q_c is the vertical leachate flux through the composite liner, which is given by:

$$q_c = n_w Q_s \tag{23}$$

being n_w the number of damaged wrinkles per unit area.

The expressions of the contaminant mass fluxes that cross the geosynthetic clay liner, $J_{s,g}$, and the attenuation layer, $J_{s,a}$, in correspondence to the wetted surface of the barrier have to take into account both the advective and the diffusive transport mechanisms and, in the specific case of the GCL, the effect which is related to the semipermeable membrane behaviour [24, 27]:

$$J_{s,g} = \left(1-\omega_g\right) q_w \frac{c_p \exp\left(P_{L,g}\right) - c_b}{\exp\left(P_{L,g}\right) - 1} \tag{24}$$

$$J_{s,a} = q_w \frac{c_b \exp\left(P_{L,a}\right) - c_x}{\exp\left(P_{L,a}\right) - 1} \tag{25}$$

where c_x is the pollutant concentration in the aquifer beneath the landfill, $P_{L,g}$ and $P_{L,a}$ are the Peclet numbers of the GCL and the AL, respectively, and q_w is the vertical leachate flux that occurs in correspondence to the wetted surface of the barrier:

$$P_{L,g} = \frac{q_w H_g}{n_g D_g^*} \tag{26}$$

$$P_{L,a} = \frac{q_w H_a}{n_a D_a^*} \tag{27}$$

398 $$q_w = \frac{Q_s}{2L_w\xi_w} \tag{28}$$

399 being D_g^* and D_a^* the effective diffusion coefficients of the contaminant in the GCL and the AL,
400 respectively, which are calculated as the product of the matrix tortuosity factor and the free-solution
401 diffusion coefficient of the contaminant [25], n_g and n_a the porosities of the GCL and the AL,
402 respectively, and H_a the thickness of the AL.

403 The balance equation for the contaminant mass flux inside the aquifer can be expressed as
404 follows:

405 $$H_{aq}\frac{\mathrm{d}}{\mathrm{d}x}\left(q_x c_x\right) = \frac{q_c}{q_w}J_{s,a} \tag{29}$$

406 Neglecting the variation in the leachate volumetric flux with respect to the x coordinate,
407 substitution of Equation 25 into Equation 29 yields the following first order linear differential
408 equation:

409 $$\frac{\mathrm{d}c_x}{\mathrm{d}x} + \chi\frac{q_c}{q_{x0}H_{aq} + q_c x}c_x = \chi\frac{q_c}{q_{x0}H_{aq} + q_c x}c_b \tag{30}$$

410 where the dimensionless χ parameter is given by:

411 $$\chi = \frac{\exp\left(P_{L,a}\right)}{\exp\left(P_{L,a}\right) - 1} \tag{31}$$

412 The relationship that exists between c_x and c_b stems from the condition of continuity in the
413 contaminant mass flux through all the mineral layers of the system (i.e. $J_{s,g} = J_{s,a}$):

414 $$c_x = A\cdot c_b - B\cdot c_p \tag{32}$$

415 where the dimensionless A and B parameters are given by:

$$A = \left(1-\omega_g\right)\frac{\exp\left(P_{L,a}\right)-1}{\exp\left(P_{L,g}\right)-1}+\exp\left(P_{L,a}\right) \tag{33}$$

$$B = \left(1-\omega_g\right)\frac{\exp\left(P_{L,a}\right)-1}{\exp\left(P_{L,g}\right)-1}\exp\left(P_{L,g}\right) \tag{34}$$

Hence, Equation 30 can be reformulated as follows:

$$\frac{\mathrm{d}c_x}{\mathrm{d}x}+\left(1-\frac{1}{A}\right)\chi\frac{q_c}{q_{x0}H_{aq}+q_c x}c_x = \frac{B}{A}\chi\frac{q_c}{q_{x0}H_{aq}+q_c x}c_p \tag{35}$$

Equation 35 is solved in conjunction with the following boundary condition:

$$c_x\left(x=0\right)=c_{x0} \tag{36}$$

where c_{x0} is the contaminant concentration in the groundwater just upstream from the landfill.

The relationship which defines the distribution of the contaminant concentration beneath the landfill can be derived under the hypothesis that the variation in the reflection coefficient with respect to the x coordinate is negligible:

$$RC = \frac{c_p\dfrac{B}{A-1}-c_{x0}}{c_p-c_{x0}}\left[1-\left(\frac{q_{x0}H_{aq}}{q_{x0}H_{aq}+q_c x}\right)^{\chi-\frac{\chi}{A}}\right] \tag{37}$$

where the parameters A, B, χ and q_c are calculated at $x = 0$ and RC is the relative contaminant concentration:

$$RC = \frac{c_x-c_{x0}}{c_p-c_{x0}} \tag{38}$$

The use of Equation 37 requires the leachate flow rate, Q_s, in correspondence to a single damaged wrinkle to be calculated though Equation 13 which, in turn, depends on the pressure head

at the bottom of the GCL. Therefore, the condition of continuity in the volumetric liquid flux through all the mineral layers of the system has to be imposed:

$$\frac{Q_s}{2L_w\xi_w} = k_a \frac{H_a + h_b - h_{aq}}{H_a} \tag{39}$$

where k_a is the hydraulic conductivity of the AL and h_{aq} is the pressure head at the bottom of the AL.

Following a rearrangement of Equation 39, the pressure head at the bottom of the GCL results to be given by:

$$h_b = h_{aq} - H_a + \frac{H_a}{H_g}\frac{k_g}{k_a}\left\{\frac{b_w}{\xi_w}\left(h_p + G\right) + \frac{G}{\xi_w\alpha}\sinh\left[\alpha\left(\xi_w - b_w\right)\right]\right\} \tag{40}$$

Finally, the practical significance of the derived analytical solutions is clarified with the aid of an example analysis. The composite liner system tested by AbdelRazek and Rowe [2] (smooth 2 mm-thick LLDPE GM + polymer-enhanced GCL) is considered for the example calculation: the fundamental fabric parameter of the GCL (i.e. the average number of lamellae per tactoid, $N_{l,AV}$) is set equal to 7.21, as detailed in the previous section of the paper, and the GM-GCL interface transmissivity is hypothesised to vary according to Equation 21. The inorganic contaminant of interest is supposed to be NaCl ($D_{Na,0}$ = 13.3·10^{-10} m^2/s, $D_{Cl,0}$ = 20.3·10^{-10} m^2/s, $D_{NaCl,0}$ = 16.1·10^{-10} m^2/s), the height of the ponded leachate in the leachate collection and removal system, h_p, is set equal to 0.5 m and the absolute temperature equal to 293.15 K. The aquifer beneath the landfill is assumed to be characterised by a thickness H_{aq} = 3 m, a length l_{aq} = 500 m, a pressure head in correspondence to the bottom of the attenuation layer h_{aq} = 1 m, a horizontal volumetric flux and a contaminant concentration in the groundwater just upstream from the landfill q_{x0} = 1·10^{-6} m/s (31.6 m/year) and c_{x0} = 0. The physical, hydraulic and transport parameters that are assigned to the geomembrane and the mineral layers are listed in Table 3.

454 The calculation results, which are reported in Figure 7 in terms of the relative contaminant
455 concentration in the groundwater just downstream from the landfill, refer to two different values of
456 the bentonite void ratio (i.e. e = 3.33 - 4.27) that are obtained as mean values of the void ratios
457 measured by AbdelRazek and Rowe [2] for each of the two considered stress levels (i.e. σ_v = 10 -
458 150 kPa). The height of the GCL is then determined as follows [34]:

459 $$H_g = \frac{m}{\rho_{sk}\left(1+w\right)}\left(1+e\right) \tag{41}$$

460 where m is the mass of bentonite per unit area in the GCL (m = 5300 g/m^2) and w is the initial water
461 content of the bentonite (w = 11%).

462 In addition to the beneficial effect of a decrease in the bentonite void ratio, which is induced
463 by an increase in the vertical load acting on the landfill bottom liner, it is shown that the
464 contribution of the osmotic phenomena in the geosynthetic clay liner can lead to a relevant
465 improvement in the containment performance of the considered barrier compared to the case of
466 absence of membrane behaviour, especially at low concentration of the contaminant in the waste
467 leachate. As a result, neglecting such a contribution can lead to an overestimation of the impact of
468 contaminant migration on the groundwater quality.

469

470 **CONCLUSIONS**

471 The bentonite semipermeable properties can affect the leakage rate through landfill composite
472 liners that consist of a GM over a GCL, as a consequence of the chemico-osmotic counter-flow that
473 is generated in response to a gradient in the contaminant concentration. The existing analytical
474 solutions, which refer to the case of a single damaged wrinkle of infinite length in the GM layer,
475 have been extended in order to account for the aforementioned osmotic phenomena, thus
476 highlighting the reduction in the liquid flow rate and the widening of the wetted area of the barrier

477 that are determined by an increase in the osmotic head. Such an extension is limited in terms of the
478 maximum value that can be assumed by the osmotic head, and further research is warranted in order
479 to investigate the effect of a larger chemico-osmotic counter-flow, until the limiting case of an
480 inversion in the direction of the overall liquid flow.

481 Furthermore, the influence of the physico-chemical interactions that take place in the
482 bentonite pores on the hydraulic transmissivity of the GM-GCL interface has been explored. The
483 results of the laboratory tests performed by AbdelRazek and Rowe [2] have been interpreted in light
484 of a constitutive model that allows the swelling-shrinking behaviour of active clays to be accounted
485 for, showing that the ability of the bentonite to swell and conform to the irregularities of the GM-
486 GCL interface, upon permeation with diluted solutions, is effective to maintain a low hydraulic
487 transmissivity. A first tentative empirical equation, valid for the tested composite liner system, has
488 been proposed in order to relate the interface transmissivity to the bentonite swelling pressure.

489 Finally, a novel analytical solution has been developed for the evaluation of the distribution of
490 the contaminant concentration within an aquifer that underlies a waste disposal facility, including
491 the influence of the semipermeable properties of the mineral layer, which is supposed to consists of
492 a GCL, on the transport rate of inorganic pollutants through the landfill composite liner. The
493 derivation of such an analytical solution is possible under the assumption that the variation in the
494 vertical leachate flux coming from the landfill, as well as in the GCL reflection coefficient, with
495 respect to the horizontal distance is negligible: this assumption is certainly acceptable when
496 diffusion represents the main transport mechanism of contaminants through the landfill liner, as in
497 the case of the low-permeability GCLs, and the groundwater seepage velocity is sufficiently high.
498 The proposed analysis approach considers steady-state conditions and a constant source
499 concentration in the leachate collection and removal system and, therefore, it represents a useful
500 tool for a preliminary evaluation of the risk related to a given contaminant concentration in the

501 waste leachate, similarly to a tier-2 risk assessment of the ASTM RBCA standard [3] for a polluted
502 site.

503

504 **REFERENCES**

505 1. AbdelRazek AY, Rowe RK (2019a) Interface transmissivity of conventional and
506 multicomponent GCLs for three permeants. Geotextiles and Geomembranes 47(1): 60–74
507 2. AbdelRazek AY, Rowe RK (2019b) Performance of GCLs in high salinity impoundment
508 applications. Geosynthetics International, accepted for publication
509 3. ASTM (2015) E2081-00: Standard guide for risk-based corrective action. ASTM
510 International, West Conshohocken, PA, USA
511 4. Di Maio C (1996) Exposure of bentonite to salt solution: osmotic and mechanical effects.
512 Géotechnique 46(4): 695–707
513 5. Dominijanni A, Manassero M (2005) Modelling osmosis and solute transport through clay
514 membrane barriers. In: Proceedings Geo-Frontiers Congress, Austin, Texas (USA), pp 349–
515 360
516 6. Dominijanni A, Manassero M (2012a) Modelling the swelling and osmotic properties of clay
517 soils. Part I: The phenomenological approach. International Journal of Engineering Science
518 51: 32–50
519 7. Dominijanni A, Manassero M (2012b) Modelling the swelling and osmotic properties of clay
520 soils. Part II: The physical approach. International Journal of Engineering Science 51: 51–73
521 8. Dominijanni A, Manassero M (2019) Steady-state analysis of pollutant transport to assess
522 landfill liner performance. Environmental Geotechnics, accepted for publication
523 9. Dominijanni A, Manassero M, Vanni D (2006) Micro/macro modeling of electrolyte transport
524 through semipermeable bentonite layers. In: Proceedings 5th International Congress on
525 Environmental Geotechnics, Cardiff, Wales (UK), vol 2, pp 1123–1130

526 10. Dominijanni A, Manassero M, Puma S (2013) Coupled chemical-hydraulic-mechanical
527 behaviour of bentonites. Géotechnique 63(3): 191–205
528 11. Dominijanni A, Manassero M, Boffa G, Puma S (2017) Intrinsic and state parameters
529 governing the efficiency of bentonite barriers for contaminant control. In: Proceedings
530 International Workshop on Advances in Laboratory Testing and Modelling of Soils and
531 Shales, Villars-sur-Ollon, Switzerland, pp 45–56
532 12. Dominijanni A, Guarena N, Manassero M (2018) Laboratory assessment of semipermeable
533 properties of a natural sodium bentonite. Canadian Geotechnical Journal 55(11): 1611–1631
534 13. Dominijanni A, Fratalocchi E, Guarena N, Manassero M, Mazzieri F (2019) Critical issues in
535 the determination of the bentonite cation exchange capacity. Géotechnique Letters 9(3): 205–
536 210
537 14. Foose GJ (2010) A steady-state approach for evaluating the impact of solute transport through
538 composite liners on groundwater quality. Waste Management 30(8–9): 1577–1586
539 15. Foose GJ, Benson CH, Edil TB (2001) Predicting leakage through composite landfill liners.
540 Journal of Geotechnical and Geoenvironmental Engineering 127(6): 510–520
541 16. Giroud JP (1997) Equations for calculating the rate of liquid migration through composite
542 liners due to geomembrane defects. Geosynthetics International 4(3-4): 335–348
543 17. Giroud JP (2016) The fifth Victor De Mello Lecture: Leakage control using geomembrane
544 liners. Soils and Rocks 39(3): 213–235
545 18. Giroud JP, Bonaparte R (1989a) Leakage through liners constructed with geomembranes -
546 Part I. Geomembrane liners. Geotextiles and Geomembranes 8(1): 27–67
547 19. Giroud JP, Bonaparte R (1989b) Leakage through liners constructed with geomembranes -
548 Part II. Composite liners. Geotextiles and Geomembranes 8(2): 71–111
549 20. Giroud JP, Touze-Foltz N (2005) Equations for calculating the rate of liquid flow through
550 geomembrane defects of uniform width and finite or infinite length. Geosynthetics
551 International 12(4): 191–204

552 21. Guyonnet D, Perrochet P, Côme B, Seguin JJ, Parriaux A (2001) On the hydro-dispersive
553 equivalence between multi-layered mineral barriers. Journal of Contaminant Hydrology 51(3–
554 4): 215–231
555 22. Liu L (2013) Prediction of swelling pressures of different types of bentonite in dilute
556 solutions. Colloids and Surfaces A: Physicochemical and Engineering Aspects 434: 303–318
557 23. Malusis MA, Scalia J, Norris AS, Shackelford CD (2019) Effect of chemico-osmosis on
558 solute transport in clay barriers. Environmental Geotechnics, accepted for publication
559 24. Manassero M (2019) The second ISSMGE Kerry Rowe Lecture: On the intrinsic, state and
560 fabric parameters of active clays for contaminant control. Canadian Geotechnical Journal,
561 accepted for publication
562 25. Manassero M, Shackelford CD (1994) The role of diffusion in contaminant migration through
563 soil barriers. Rivista Italiana di Geotecnica 28(1): 5–31
564 26. Manassero M, Dominijanni A (2010) Coupled modelling of swelling properties and
565 electrolyte transport through geosynthetic clay liners. In: Proceedings 6th International
566 Congress on Environmental Geotechnics, New Delhi, India, vol 1, pp 260–271
567 27. Manassero M, Benson CH, Bouazza A (2000) Solid waste containment systems. In:
568 Proceedings GeoEng 2000, Melbourne, Australia, vol 1, pp 520–642
569 28. Manassero M, Dominijanni A, Fratalocchi E, Mazzieri F, Pasqualini E, Boffa G (2016) About
570 the state parameters of active clays. In: Geoenvironmental Engineering: Honoring David E.
571 Daniel, Chicago, Illinois (USA), pp 99–110
572 29. Manassero M, Dominijanni A, Guarena N (2018) Modelling hydro-chemo-mechanical
573 behaviour of active clays through the fabric boundary surface. In: Proceedings China-Europe
574 Conference on Geotechnical Engineering, Vienna, Austria, pp 1618–1626
575 30. Mendes MJA, Touze-Foltz N, Palmeira EM, Pierson P (2010) Influence of structural and
576 material properties of GCLs on interface flow in composite liners due to geomembrane
577 defects. Geosynthetics International 17(1): 34–47

578 31. Musso G, Cosentini RM, Dominijanni A, Guarena N, Manassero M (2017) Laboratory
579 characterization of the chemo-hydro-mechanical behaviour of chemically sensitive clays.
580 Rivista Italiana di Geotecnica 51(3): 22–47
581 32. Muurinen A, Carlsson T, Root A (2013) Bentonite pore distribution based on SAXS, chloride
582 exclusion and NMR studies. Clay Minerals 48(2): 251–266
583 33. Olson RE, Mesri G (1970) Mechanisms controlling the compressibility of clays. Journal of
584 the Soil Mechanics and Foundations Division, ASCE, 96(6): 1863–1878
585 34. Petrov RJ, Rowe RK (1997) Geosynthetic clay liner (GCL) – chemical compatibility by
586 hydraulic conductivity testing and factors impacting its performance. Canadian Geotechnical
587 Journal 34(6): 863-885
588 35. Rowe RK (1998) Geosynthetics and the minimization of contaminant migration through
589 barrier systems beneath solid waste. In: Proceedings of the 6th International Conference on
590 Geosynthetics, Atlanta, GA, USA, pp 27–103
591 36. Rowe RK (2005) Long-term performance of contaminant barrier systems. 45th Rankine
592 Lecture. Géotechnique 55(9): 631–678
593 37. Rowe RK (2012) Short and long-term leakage through composite liners. 7th Arthur
594 Casagrande Lecture. Canadian Geotechnical Journal 49(2): 141–169
595 38. Rowe RK, Abdelatty K (2013) Leakage and contaminant transport through a single hole in
596 the geomembrane component of a composite liner. Journal of Geotechnical and
597 Geoenvironmental Engineering 139(3): 357–366
598 39. Shackelford CD (2014) The ISSMGE Kerry Rowe Lecture: The role of diffusion in
599 environmental geotechnics. Canadian Geotechnical Journal 51(11): 1219–1242
600 40. Sposito G (2016) The chemistry of soils. Oxford University Press, United Kingdom
601 41. Tournassat C, Appelo CAJ (2011) Modelling approaches for anion-exclusion in compacted
602 Na-bentonite. Geochimica et Cosmochimica Acta 75: 3698–3710

603 42. Touze-Foltz N, Giroud JP (2003) Empirical equations for calculating the rate of liquid flow
604 through composite liners due to geomembrane defects. Geosynthetics International 10(6):
605 215–233
606 43. Touze-Foltz N, Rowe RK, Duquennoi C (1999) Liquid flow through composite liners due to
607 geomembrane defects: analytical solutions for axi-symmetric and two-dimensional problems.
608 Geosynthetics International 6(6): 455–479

609

Table 1 Interpretation of the results of the hydraulic conductivity tests performed by AbdelRazek and Rowe [2] on a polymer-enhanced GCL. Note: the void ratio has been calculated, under the hypothesis of complete saturation, adopting a specific gravity of the bentonite G_s = 2.65 [12].

Test ID	Ionic strength	Hydraulic conductivity	Water content	Void ratio	Average number of lamellae per tactoid
	[mM]	[m/s]	[%]	[-]	[-]
GCg1m-SA2-10	4400	$2 \cdot 10^{-10}$	153	4.05	12.46
GCg1m-SB1-10	4400	$2 \cdot 10^{-10}$	159	4.21	11.81
GCg1m-SD1-150	4400	$2 \cdot 10^{-11}$	125	3.31	6.08
GCg1m-SE1-150	4400	$4 \cdot 10^{-11}$	125	3.31	8.13
GCg1m-SE2-150	4400	$3 \cdot 10^{-11}$	128	3.39	6.94
GCg1m-SA2-150 [a]	4400	$2 \cdot 10^{-11}$	137	3.63	5.31
GCg1m-SP1-10-10%	440	$1 \cdot 10^{-10}$	135	3.58	10.85
GCg1m-SZ-10-RO [a]	< 3.29	$1 \cdot 10^{-11}$	187	4.96	2.64
GCg1m-SQ1-150-50%	2200	$1 \cdot 10^{-11}$	125	3.31	4.64
GCg1m-SR2-150-10%	440	$5 \cdot 10^{-12}$	121	3.21	3.80
GCg1m-SP1-150-10% [a]	440	$4 \cdot 10^{-11}$	115	3.05	9.25
GCg1m-SZ-150-RO [a]	< 3.29	$1.5 \cdot 10^{-11}$	139	3.68	4.63

[a] As the water content was not indicated for these GCL specimens, it was estimated on the basis of the values reported for similar specimens tested under the same vertical stress and ionic strength of the permeant.

Table 2 Interpretation of the results of the interface transmissivity tests performed by AbdelRazek and Rowe [2] on a composite liner system, which consists of a smooth LLDPE GM overlying a polymer-enhanced GCL. Note: the average number of lamellae per tactoid has been assumed equal to the arithmetic mean of the values reported in Table 1 ($N_{l,AV}$ = 7.21).

Test ID	Ionic strength	Vertical stress	Steady-state interface transmissivity	Water content	Void ratio	Swelling pressure
	[mM]	[kPa]	[m^2/s]	[%]	[-]	[kPa]
GCg1m-SJ1-BxV20-10-RO	3	10	$4.9 \cdot 10^{-11}$	187	4.96	18.37
GCg1m-SL1-BxV20-150-RO	3	150	$1.3 \cdot 10^{-11}$	139	3.68	32.36
GCg1m-SA1-BxV20-10	4400	10	$3.3 \cdot 10^{-10}$	169	4.48	0.03
GCg1m-SA2-BxV20-10	4400	10	$1.7 \cdot 10^{-10}$	153	4.05	0.04
GCg1m-SP1-BxV20-10-10%	440	10	$2.1 \cdot 10^{-10}$	135	3.58	0.51
GCg1m-SD1-BxV20-150	4400	150	$2 \cdot 10^{-10}$	125	3.31	0.06
GCg1m-SD2-BxV20-150	4400	150	$9.5 \cdot 10^{-11}$	137	3.63	0.05
GCg1m-SQ1-BxV20-150-50%	2200	150	$5.3 \cdot 10^{-10}$	125	3.31	0.13
GCg1m-SQ2-BxV20-150-50%	2200	150	$3.3 \cdot 10^{-10}$	115	3.05	0.17
GCg1m-SO1-BxV20-150-50%	2200	150	$1 \cdot 10^{-10}$	128	3.39	0.12
GCg1m-SP2-BxV20-150-10%	440	150	$1.7 \cdot 10^{-11}$	115	3.05	0.84
GCg1m-SR2-BxV20-150-10%	440	150	$3.6 \cdot 10^{-11}$	121	3.21	0.71

14 **Table 3** Physical, hydraulic and transport parameters of the geomembrane and the mineral layers of

15 the example landfill bottom liner.

Parameter	Mineral layers	
	GCL	**AL**
Thickness, H (m)	0.0078 - 0.0095	2
Hydraulic conductivity, k (m/s)	Equation 19	$1 \cdot 10^{-7}$
Void ratio, e	3.33 - 4.27	0.43
Matrix tortuosity, τ_m	0.2	0.25
	Geomembrane	
Wrinkle length, L_w (m)	200	
Wrinkle width, $2b_w$ (m)	0.2	
Number of wrinkles per hectare, n_w (1/ha)	1	

16

17

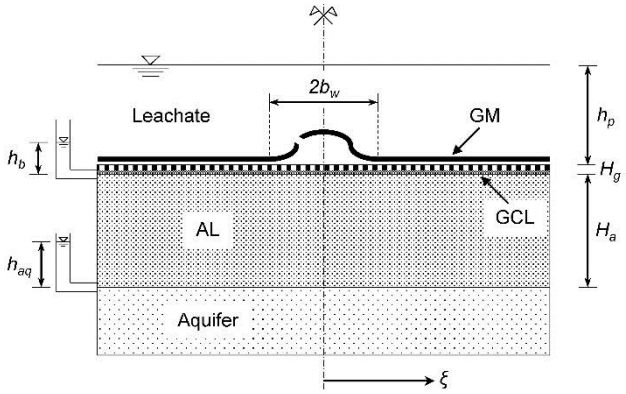

1

2 **Figure 1** Reference scheme for the calculation of the leachate flow rate through a composite liner

3 which consists of a GM overlying a GCL.

4

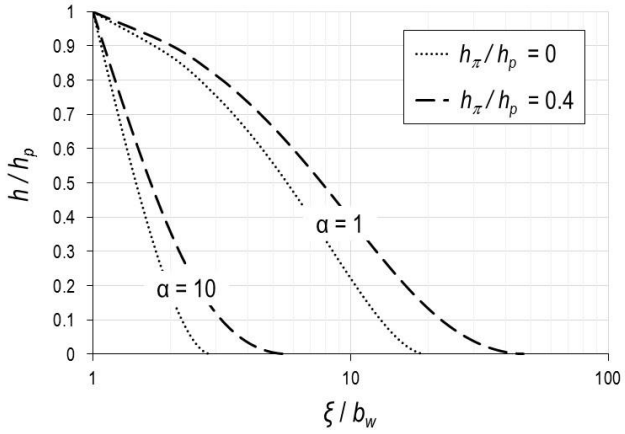

5

6 **Figure 2** Influence of the GCL osmotic properties and of the α parameter on the pressure head

7 distribution in the GM-GCL interface (b_w = 0.1 m, h_p = 0.5 m, H_g = 0.01 m, h_b = -0.2 m).

8

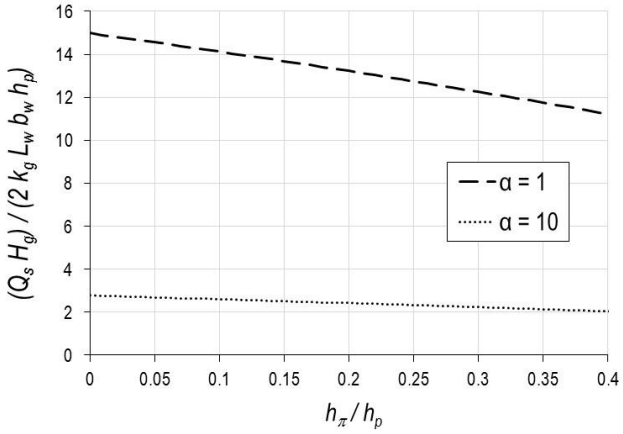

9

10 **Figure 3** Influence of the GCL osmotic properties and of the α parameter on the liquid flow rate

11 through a single damaged wrinkle (b_w = 0.1 m, h_p = 0.5 m, H_g = 0.01 m, h_b = -0.2 m).

12

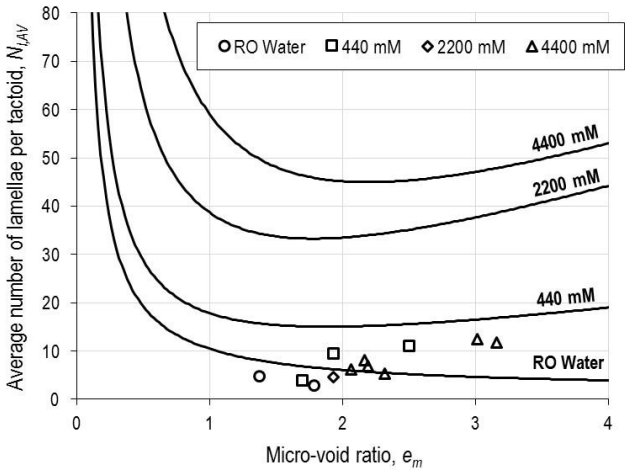

Figure 4 Comparison between the values of the average number of lamellae per tactoid, as obtained through the interpretation of the results of the hydraulic conductivity tests that were performed by AbdelRazek and Rowe [2] on a polymer-enhanced GCL (open symbols), and the iso-concentration curves of the Fabric Boundary Surface, as calibrated on the results of the hydraulic conductivity tests that were performed by Petrov and Rowe [34] on an untreated needle-punched GCL (continuous lines).

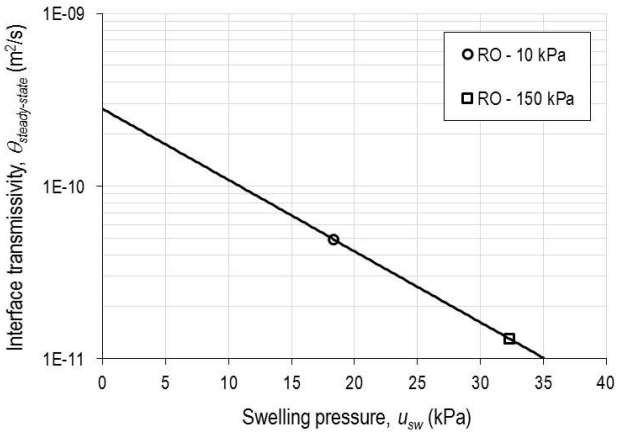

21

22 **Figure 5** Steady-state values of the GM-GCL interface transmissivity measured by AbdelRazek and
23 Rowe [2] with reverse osmosis water as a function of the calculated swelling pressure (open
24 symbols), together with the interpolation curve (continuous line).

25

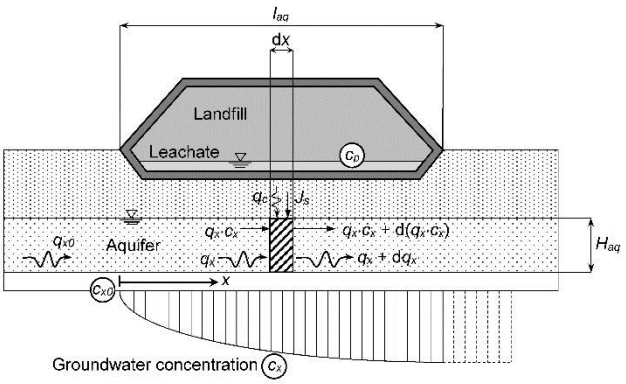

26

27 **Figure 6** Reference scheme for the water volumetric balance and the contaminant mass balance

28 within a thin aquifer beneath the landfill (modified from Dominijanni and Manassero [8]).

29

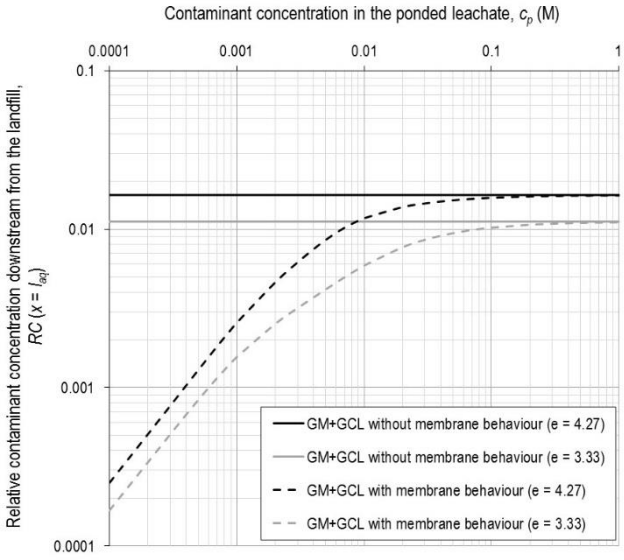

30

31 **Figure 7** Effectiveness of the composite liner tested by AbdelRazek and Rowe [2] in limiting the
32 contaminant migration from the landfill towards the underlying aquifer, taking into account the
33 improvement in the containment performance due to the semipermeable membrane behaviour of the
34 GCL.

35